american physiological society

JNP JOURNAL OF NEUROPHYSIOLOGY

J Neurophysiol 135: 579–589, 2026.
First published January 30, 2026; doi:10.1152/jn.00240.2025

RESEARCH ARTICLE

Control of Movement

Weight-bearing symmetry changes after asymmetric surface stiffness walking

Mark Price,[1,2]* Elena G. Schell,[1]* Jonaz Moreno Jaramillo,[1] Jenna M. Chiasson,[1] Leah C. Metsker,[3] Meghan E. Huber,[2,4] and Wouter Hoogkamer[1,4]

[1]*Department of Kinesiology, University of Massachusetts Amherst, Massachusetts, United States;* [2]*Department of Mechanical and Industrial Engineering, University of Massachusetts Amherst, Massachusetts, United States;* [3]*Department of Biomedical Engineering, University of Massachusetts Amherst, Massachusetts, United States; and* [4]*Center for Personalized Health Monitoring, Institute for Applied Life Sciences, University of Massachusetts Amherst, Massachusetts, United States*

Abstract

Mechanical gait asymmetry is a prevalent deficit in many forms of locomotion impairment. Although spatial gait asymmetry adaptations can be elicited with split-belt treadmill training, weight-bearing and propulsion asymmetry remain resistant to improvement. As an alternative approach, we tested asymmetric surface stiffness walking to induce neuromotor adaptation of weight-bearing and propulsion asymmetries. We hypothesized that a bout of asymmetric stiffness walking would elicit aftereffects in the form of asymmetries in weight bearing, propulsion, and plantar flexor activity. Twelve healthy young adults performed a 10-min bout of asymmetric stiffness walking on an adjustable stiffness treadmill. We measured baseline and postperturbation ground reaction forces (GRFs) and spatiotemporal measures during 5-min walking bouts on a dual-belt instrumented treadmill. After asymmetric surface stiffness walking, participants exhibited 2.8% asymmetry in vertical GRF at push off, as well as increased plantarflexor muscle activity (20.7% GAS, 9.5% SOL) during push off on the perturbed side relative to the unperturbed. Participants also decreased their midstance vertical GRF (2.2%) and increased their peak braking GRF (6.8%) on the perturbed side relative to unperturbed. Counter to our hypothesis, they did not increase their propulsion GRF on the perturbed side. We conclude that asymmetric stiffness walking elicited a neuromotor adaptation toward a relative increase in push-off in the target limb, albeit primarily vertically aligned in our cohort of healthy young adults, and that gait adaptation to asymmetric stiffness walking should be investigated in individuals with push-off asymmetries.

NEW & NOTEWORTHY Weight-bearing asymmetry in individuals with hemiparetic stroke is resistant to treatments that produce improvements in other gait function measures (e.g., spatiotemporal symmetry). We investigated a novel perturbed ground stiffness intervention applied by an adjustable surface stiffness treadmill and found significant aftereffects in vertical and braking ground reaction force peaks in healthy young adults, as well as increases in perturbed-side plantar flexor activity during push-off, indicating a strong potential for correcting persistent deficiencies in poststroke gait.

aftereffects; hemiparesis; motor adaptation; split-belt walking; stiffness perturbation

INTRODUCTION

Gait asymmetries are common in many neurological and musculoskeletal conditions, such as hemiparetic stroke (1), Parkinson's disease (2), multiple sclerosis (3), anterior cruciate ligament injury (4), and osteoarthritis (5). Although gait asymmetries visually present as spatial (e.g., step length asymmetry) or temporal (e.g., stance time asymmetry), mechanical asymmetries (e.g., asymmetries in ground reaction force) can limit mobility (6) and can increase risks for secondary musculoskeletal conditions such as osteoarthritis on the overused side (7) and osteoporosis on the underused side (8). It is well understood that reduced mobility is a primary limiter of activities of daily living and quality of life (9). Thus, understanding the mechanisms that underlie motor adaptation in mechanical asymmetries is imperative.

Split-belt treadmill training is a recent form of physical therapy shown to effectively reduce spatial gait asymmetries

*M. Price and E. G. Schell contributed equally to this work.
Correspondence: M. Price (mprice@umass.edu).
Submitted 16 May 2025 / Revised 7 September 2025 / Accepted 25 January 2026

0022-3077/26 Copyright © 2026 The Authors. Licensed under Creative Commons Attribution CC-BY-NC-ND 4.0.
Published by the American Physiological Society.

Downloaded from journals.physiology.org/journal/jn at Univ of Massachusetts (128.119.077.226) on October 26, 2026.

(10). In split-belt treadmill training, a participant walks on a treadmill with two belts, one for each leg. The belt speeds are different, set to exaggerate the asymmetry in step length, which drives neuromotor adaptation toward less asymmetric step lengths after exposure (11). Although repetitive bouts of such short-term adaptation lead to longer-term improvements in spatial gait asymmetry (10), a major shortcoming of current split-belt treadmill training protocols is that they do not reduce temporal asymmetries that result from asymmetries in weight-bearing and propulsion forces (12, 13). Alternatively, real-time audiovisual biofeedback displaying real-time propulsive ground reaction forces (GRFs) or trailing limb angles can improve propulsion (14, 15), but the benefits of such explicit learning interventions might not result in long-lasting benefits as observed for implicit learning interventions (16).

Asymmetric surface stiffness treadmill walking has been shown to change gait patterns in healthy individuals using implicit locomotor adaptation principles similar to those observed in split-belt treadmill walking (17). In this paradigm, rather than exposing participants to asymmetrical belt speeds, they are instead exposed to asymmetrical ground stiffness, during which the platform under one foot deflects downward in response to walking loads (17). Because the perturbation in this case is responsive to the limb-loading dynamics of gait, it is theorized that it could elicit adaptations to weight-bearing and propulsion force symmetry. Encouragingly, vertical GRF during push-off seemed to increase by 17% in healthy young adults after asymmetric stiffness walking (17), although reported vertical GRF values were lower than typically observed (18). Despite these preliminary results, it is unclear if weight-bearing or propulsion symmetry is affected by asymmetric stiffness walking, as vertical GRFs were measured only for one side, and propulsion GRFs were not measured at all. Furthermore, while muscle activity was measured, it was calculated only for the swing phase of walking, despite changes in plantar flexor activity during push-off being of critical importance for determining the promise of this technique for addressing hemiparetic deficits (6). There is thus a critical need to quantify neuromotor adaptation to asymmetric stiffness walking in vertical and horizontal GRFs, muscle activity, and spatiotemporal gait parameters.

This study aims to *1*) quantify the bilateral effects of neuromotor adaptation to an asymmetric stiffness walking intervention in measures relevant to common mobility-related gait disorders (e.g., stroke), and *2*) understand mechanisms that underlie how asymmetric stiffness walking produces aftereffects in weight bearing and muscle activity in healthy individuals. Extrapolating from the preliminary findings by Chambers and Artemiadis (17), we hypothesize that after a single bout of asymmetric surface stiffness walking, vertical (vGRF) and propulsive ground reaction forces (pGRF), and stance time will increase on the low stiffness side relative to the unperturbed side. Corresponding with these changes, we hypothesize that gastrocnemius and soleus muscle excitation will increase during push-off on the low-stiffness side relative to the unperturbed side. We also hypothesize that tibialis anterior activity will increase during the swing phase on the unperturbed side due to the increased relative height of the rigid treadmill during stance on the low-stiffness side. In addition to testing these hypotheses, we performed a holistic analysis of GRF and EMG measures.

METHODS

Participants

Twelve healthy young individuals participated in this study (21 ± 1 yr, 69.3 ± 8.1 kg, 164 ± 7 cm, 11 F/1M). All participants were free of musculoskeletal or neurological injury, disease, or surgery that would affect gait or balance behavior. They were capable of walking at a comfortable pace for 30 consecutive minutes and had no prior experience walking on an asymmetric surface stiffness treadmill. Participants gave their written informed consent in accordance with the ethical guidelines of the UMass Amherst Institutional Review Board (Protocol 5248).

AdjuSST

The AdjuSST (Adjustable Surface Stiffness Treadmill) is our custom-built dual-belt treadmill with one belt operating around a rigid platform and the other belt around a platform resting atop a leaf spring mechanism, allowing for vertical deflection under weight (19). For this study, we operated the adjustable side in two settings: rigid (300 kN/m) and compliant (15 kN/m). In the compliant setting, under a static load of 750 N (~75 kg), the belt displaces 50 mm downward. Mechanical stops with shock-absorbing foam prevent movement beyond 100 mm. We set the perturbed side to the right or left by specifying the walking direction and running the belts in forward or reverse accordingly. The first eight participants experienced a left-side perturbation, and the final four experienced a right-side perturbation, for logistical reasons.

Protocol

Participants performed two 5-min walking trials on a force-instrumented dual-belt treadmill (Bertec, Columbus, OH), one before and one after walking a 12-min walking trial on the AdjuSST, including 10 min of walking with one leg at the rigid belt, and one leg at the compliant belt at a stiffness of 15 kN/m (Fig. 1). The 5-min walking trials allowed us to compare baseline walking kinetics and muscle activations to potential after-effects in walking kinetics and muscle activations from the motor adaptation to asymmetric surface stiffness walking.

Experimental set up before the first walking trial consisted of fitting the participant with proper sizes of shoes (Speed Sutamina, Puma, Herzogenaurach, Germany) and force measuring insoles (loadsol, Novel, Munich, Germany). We placed 10 lower limb surface electromyography (EMG) sensors (Delsys Trigno, Natick, MA) bilaterally on five lower limb muscles: vastus lateralis (VL), tibialis anterior (TA), gastrocnemius lateral head (GAS), soleus (SOL), and biceps femoris (BF). Following, we placed four markers on the participants' shoes, one on each heel, and one on each fifth metatarsal head, used for gait event detection during AdjuSST walking. Participants first performed a 5-min walking trial on the force-instrumented treadmill ("Baseline").

Downloaded from journals.physiology.org/journal/jn at Univ of Massachusetts (128.119.077.226) on October 26, 2026.

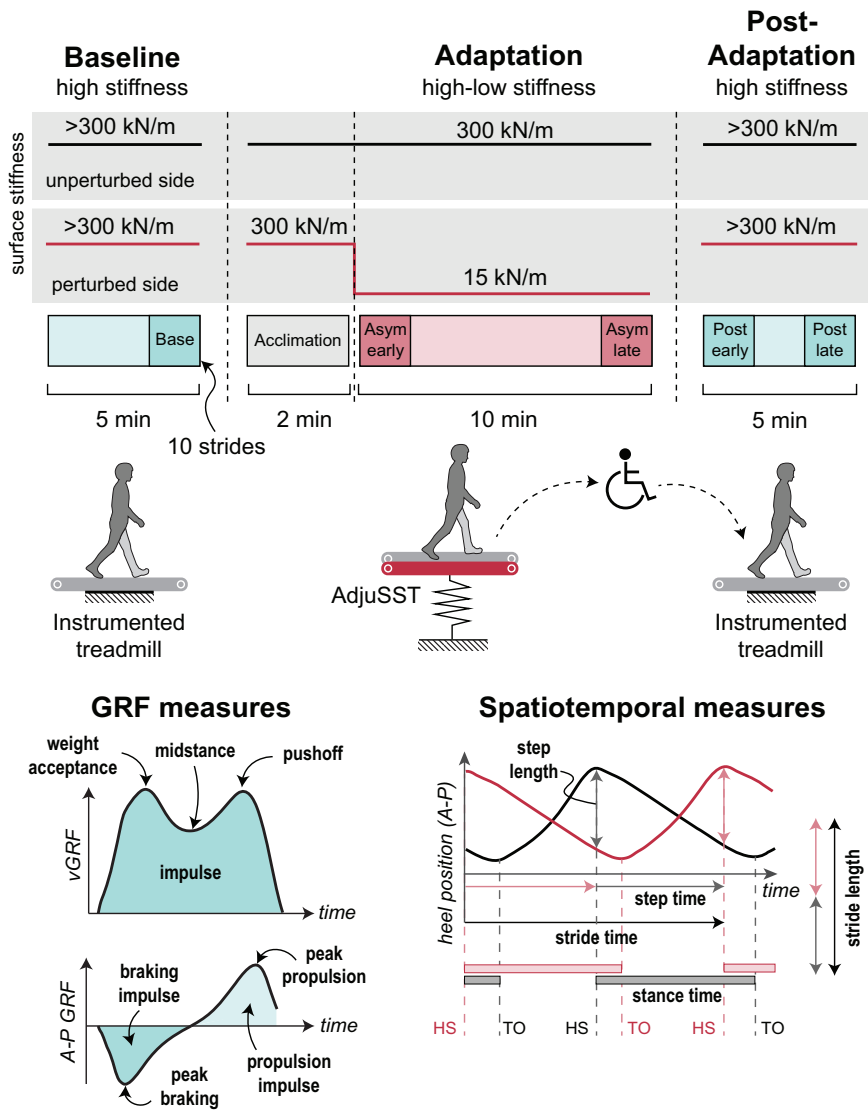

Figure 1. Experimental setup and paradigm. Participants experienced asymmetric surface stiffness walking on a custom adjustable stiffness treadmill [AdjuSST; (19)]. Experimental paradigm. Participants walked in 4 total bouts, a 5-min baseline bout on a rigid instrumented treadmill, a 2-min acclimation period on the AdjuSST with both belts kept at high stiffness, a 10-min adaptation period on the AdjuSST after the surface stiffness was abruptly lowered on one side, and a 5-min postperturbation bout on the rigid instrumented treadmill. Participants were transferred to the instrumented treadmill by wheelchair to prevent washout of adaptation effects in transit.

For all conditions, the participants walked at 1.25 m/s. We collected ground reaction force (GRF) data at 1,000 Hz, and EMG data at 1,926 Hz using QTM (Qualisys, Göteborg, Sweden) and insole force data at 100 Hz for 60 s during the final minute of the 5-min trial.

After the Baseline trial, we led participants to the AdjuSST, located in a separate laboratory space, ~60 m from the force-instrumented treadmill. Participants then completed a 12-min walking trial on the AdjuSST. For the first 2 min of this trial, both belts were set at high stiffness, similar to ground stiffness. After 2 min, one belt's stiffness condition was lowered to 15 kN/m within a single step. Participants walked for 10 min with one belt set at high stiffness and the other set at 15 kN/m. We measured EMG data at 1,926 Hz and foot marker location at 100 Hz with QTM, and insole force data at 100 Hz for 60 s during the first and final minute of these 10 min. Upon completion of the 10-min intervention condition, we stopped the treadmill and asked participants to not take any additional steps, in efforts to decrease preemptive washout of aftereffects. We then transferred participants into a wheelchair and transported them back to the force-instrumented treadmill.

Participants then performed a 5-min walking trial on the force-instrumented treadmill ("Post"), which allowed us to quantify aftereffects in gait symmetry. We collected ground reaction force (GRF) data at 1,000 Hz, and EMG data at 1,926 Hz using QTM and insole force data at 100 Hz for 60 s during the first and final minute of the 5-min trial.

Data Analysis

We smoothed ground reaction force vectors and centers of pressure obtained from the rigid instrumented treadmill with a fourth-order Butterworth low-pass filter with a cut-off frequency of 30 Hz. We identified heel strike and toe-off events for each limb as the moment in which the force vector magnitude for the corresponding force plate exceeded (heel strike) or fell beneath (toe-off) a threshold of 100 N. Gait events were manually verified for all strides, and strides in which the stance foot interacted with both force plates simultaneously were discarded. Motion capture marker

Downloaded from journals.physiology.org/journal/jn at Univ of Massachusetts (128.119.077.226) on October 26, 2026.

trajectories were smoothed with a fourth-order Butterworth low-pass filter with a cutoff frequency of 6 Hz.

Vertical ground reaction forces from the force measuring insoles were initially processed in the same manner as the force plate data from the rigid treadmill, segmented at 100 Hz. We additionally calibrated the insole measurements against the force plate measurements recorded during the baseline walking trial. We compared the vGRF trajectory averaged across 20 corresponding strides between the force plates and the insoles, then applied a gain and offset to the forefoot and hindfoot insole signals to match the peak values of the resultant vGRF with the force plate vGRF peaks, as well as to zero the insole reading during swing (Supplemental Fig. S1). The gain and offset calculated from this sample were applied to all corresponding insole measurements for the duration of the experiment, per participant.

We calculated muscle excitation profiles from the EMG signals by applying a fourth-order Butterworth band-pass filter (30–300 Hz) to eliminate noise in the signal. We then DC bias corrected, rectified, and applied a fourth-order Butterworth low-pass filter (5 Hz) to create the linear envelope for each muscle excitation signal (20, 21). EMG signals were segmented by stride at 100 Hz. We calculated the peak value of each linear envelope signal per stride, averaged the peaks for the final 10 strides of the baseline trial, and used the resulting value to scale the filtered signal for the corresponding sensor for all conditions. Because of sensor malfunctions, two of the 12 participants could not be included for any EMG analyses, and one additional participant was not included in each of the SOL and the VL analyses. We performed all experimental data processing with custom scripts using MATLAB (MathWorks, Natick, MA).

Dependent Measures

To quantify weight bearing, we calculated the first (weight acceptance) and second (pushoff) vGRF peak, the minimum vGRF during midstance, and the time integral of the vGRF profile during stance (vGRF impulse) per side, per stride. To quantify propulsion, we calculated the peak pGRF and pGRF impulse per side, per stride. We also calculated the peak and impulse of the braking ground reaction force (bGRF) per side for all strides.

To quantify spatiotemporal parameters of gait, we calculated stance time per side as the elapsed time between heel strike and subsequent toe off events. We similarly calculated step time per side as the elapsed time between the heel strike of the contralateral limb and the subsequent heel strike of the ipsilateral limb. We calculated step length as the anterior-posterior distance between heel markers at the moment of heel strike of the corresponding side. Stride time and stride length are defined as the sum of the step time or step length of both sides for a given stride.

To quantify changes in muscle activity corresponding with our hypothesized changes in weight bearing and propulsion, we calculated peak muscle excitations of the gastrocnemius and soleus during push-off (between 30 and 70% of the gait cycle) and the vastus lateralis during weight acceptance (0–20%). To further investigate changes relevant to poststroke gait (i.e., drop foot, knee hyperextension), we calculated peak excitation of the first burst of tibialis anterior activity during swing (60–80%) (22) and peak excitation of the biceps femoris during terminal swing (80–100%).

For all unilateral measures, we calculated an asymmetry ratio to indicate the relative magnitude of a measure on the perturbed versus unperturbed side. This ratio is defined as:

$$\text{Asymmetry}\,\% = \frac{X_p - X_u}{X_p + X_u} \times 100\% \quad (1)$$

where X_p is the measure calculated for the side that was perturbed with low surface stiffness, and X_u is the measure for the side that remained unperturbed. Unless otherwise specified, all statistical analyses were performed on the asymmetry ratio of the corresponding measure.

Statistical Analyses

We averaged all measures per participant in 10-stride windows to represent three experimental conditions: the final 10 strides of the baseline walking trial ("Baseline"), the initial 10 strides on the instrumented treadmill after exposure to asymmetric surface stiffness ("Post-early"), and the final 10 strides after 5 min of postperturbation walking ("Post-late"). We defined two additional conditions for measures calculated from the insoles and EMG sensors, which we were able to record during the perturbation: the first ("Asym-early") and final ("Asym-late") 10 strides of asymmetric stiffness walking.

To determine whether asymmetric stiffness walking significantly influenced a given measure, we used a one-way repeated-measures analysis of variance (ANOVA). We tested for sphericity (i.e., the assumption of equal variances of the differences between all combinations of conditions) with Mauchly's test; if the assumption of sphericity was violated, we applied the Greenhouse–Geisser correction factor to the degrees of freedom of the ANOVA. For measures with a significant effect of walking period condition, we conducted a post hoc comparison using a two-tailed paired t test between the Baseline and Post-early conditions to test our hypothesis that asymmetric walking would result in an asymmetry relative to baseline after the perturbation (see the introduction for predictions for specific measures). For measures with significant asymmetry aftereffects, we additionally conducted comparisons between Baseline and Post-early with a two-tailed paired t test for the perturbed and unperturbed sides separately. We performed all statistical analyses using MATLAB (Statistics and Machine Learning Toolbox), and the significance level was set at $\alpha = 0.05$ for all tests.

RESULTS

Weight Bearing

We found a significant effect of walking period condition in push-off ($P < 0.001$) and mid-stance ($P < 0.001$) vGRF peaks, but not during weight acceptance ($P = 0.055$) or vGRF impulse ($P > 0.1$) (Table 1 and Fig. 2). Relative to Baseline, participants had larger push-off vGRF peaks (+2.8% asymmetry, $P < 0.001$) on the perturbed side than the unperturbed side during the Post-early window (Fig. 3). This asymmetry was due both to a decrease on the unperturbed side ($P = 0.006$) and an increase on the perturbed side ($P =$

Downloaded from journals.physiology.org/journal/jn at Univ of Massachusetts (128.119.077.226) on October 26, 2026.

Table 1. *Ground reaction force and spatiotemporal outcome measures*

	Baseline	Post-Early	Post-Late	Main Effect *P* Value
Peak weight acceptance vGRF (% Asym)	−0.1 ± 1.8	0.9 ± 2.7	−0.3 ± 2.3	0.055
Peak push-off vGRF (% Asym)	**−0.1 ± 1.6**	**2.7 ± 1.0**	**0.7 ± 1.6**	**<0.001**
Min. midstance vGRF (% Asym)	**−0.3 ± 1.7**	**−2.5 ± 2.2**	**−0.2 ± 2.3**	**<0.001**
vGRF impulse (% Asym)	0.1 ± 1.5	0.7 ± 1.9	0.46 ± 1.2	0.606
Peak braking (% Asym)	**0.1 ± 5.7**	**6.9 ± 7.8**	**1.1 ± 6.1**	**0.001**
Peak propulsion (% Asym)	0.8 ± 4.1	1.9 ± 4.3	1.7 ± 3.4	0.433
Braking impulse (% Asym)	1.5 ± 5.1	1.8 ± 9.7	−0.2 ± 5.0	0.584
Propulsion impulse (% Asym)	−0.7 ± 3.6	−0.3 ± 5.4	0.84 ± 3.2	0.507
Step time (% Asym)	0.3 ± 0.8	−0.4 ± 1.6	0.1 ± 1.3	0.234
Stance time (% Asym)	0.1 ± 0.8	−0.5 ± 1.3	0.1 ± 0.8	0.174
Step length (% Asym)	0.4 ± 1.6	0.4 ± 2.6	−0.3 ± 1.3	0.433
Stride time, s	1.1 ± 0.0	1.1 ± 0.1	1.1 ± 0.1	0.662
Stride length, m	1.3 ± 0.1	1.3 ± 0.1	1.3 ± 0.1	0.979

Values are means ± SD. Significant differences ($P < 0.05$) are shown in bold. Positive asymmetry = relatively greater value on the perturbed than the unperturbed side. Negative asymmetry = relatively greater value on the unperturbed than the perturbed side.

0.034). Participants had lower mid-stance vGRF on the perturbed than the unperturbed side (−2.2% asymmetry, $P < 0.001$) in Post-early relative to Baseline. This was driven by a reduction on the perturbed side ($P < 0.001$); we did not detect a significant change on the unperturbed side ($P = 0.070$).

Propulsion and Braking

We found a significant effect of walking period condition in peak braking force ($P = 0.001$), but not peak propulsion, braking impulse, or propulsion impulse (Table 1 and Fig. 2). Relative to Baseline, participants had larger peak braking (+6.8% asymmetry, $P = 0.006$) on the perturbed than the unperturbed side during the Post-early window (Fig. 4). This was driven by an increase on the perturbed side ($P = 0.010$); we did not detect a significant change on the unperturbed side ($P > 0.1$).

Spatiotemporal

We did not find a significant effect of walking period condition on step time symmetry, stance time symmetry, or overall stride time ($P > 0.1$ for all cases) (Table 1). Likewise, we did not find a significant effect of walking period condition on step length or stride length ($P > 0.1$) (Supplemental Fig. S2).

Muscle Excitations

We found a significant effect of walking period condition on asymmetry in all five EMG measures (Table 2 and Fig. 2). Of these, GAS (+20.7% asymmetry, $P < 0.001$), SOL (+9.5% asymmetry, $P = 0.016$), and TA (−8.8% asymmetry, $P = 0.002$) showed asymmetry aftereffects relative to baseline. Both plantar flexors showed relatively higher muscle activity on the perturbed side during the post-late condition, though the TA effect was to relatively increase activity on the unperturbed side, in part canceling out a baseline asymmetry of +5.4% favoring the perturbed side (Fig. 5). Investigating the effects on individual sides, GAS activity significantly increased on the perturbed side ($P = 0.002$) and TA activity significantly increased on the unperturbed side ($P = 0.043$), but we did not detect significant changes for the unperturbed GAS ($P > 0.1$), the perturbed TA ($P > 0.1$), or the SOL for either side in isolation ($P = 0.080$ unperturbed; $P > 0.1$ perturbed).

DISCUSSION

Overall, participants presented significant weight-bearing aftereffects after exposure to asymmetric stiffness walking. In support of our hypothesis, peak push-off vGRF shifted toward the perturbed side limb along with associated muscle excitations in the plantar flexors. Counter to our hypothesis, we did not observe a significant shift in propulsion force, vGRF impulse, or stance time symmetry.

Weight-Bearing Adaptation and Aftereffects

Participants changed their weight-bearing patterns in response to the intervention, notably by shifting peak push-off toward the perturbed side by ∼3%. For comparison, individuals post stroke commonly exhibit a 10% weight-bearing asymmetry during quiet standing that persists after rehabilitation (23), though weight-bearing asymmetry data during walking is scarce. Although the mechanical effect is relatively small, we note that our participants are not affected by neurological disease or injury, and that the changes in plantarflexor activity are large in comparison (over 20% for GAS). Clinical relevance for this finding is yet to be determined.

During adaptation, the vGRF profile was distorted, losing its "double hump" shape almost completely, with the first peak increasing in magnitude and the second peak nearly disappearing (Fig. 2). Interestingly, postperturbation, the weight acceptance peak was not significantly affected while the push-off peak on the perturbed side substantially increased relative to baseline. This may indicate that the qualitatively large increase in weight acceptance vGRF during the perturbation is mainly due to the passive mechanical dynamics of asymmetric stiffness walking and did not require a major adaptation to the neuromotor control of walking. Visual analysis of per-stride weight acceptance vGRF reveals an initial asymmetry postperturbation (Fig. 3) but appears to wash out within fewer than 10 strides. This rapid washout suggests that reacclimation to a "normal" walking context occurs on a short timescale, consistent with fast adaptation rather than longer-term learning. In contrast, the reduction or disappearance of the push-off peak during the perturbation appears to have elicited compensations toward increased vertical push-off that we observed in the post-early window. In support of this explanation, we

Downloaded from journals.physiology.org/journal/jn at Univ of Massachusetts (128.119.077.226) on October 26, 2026.

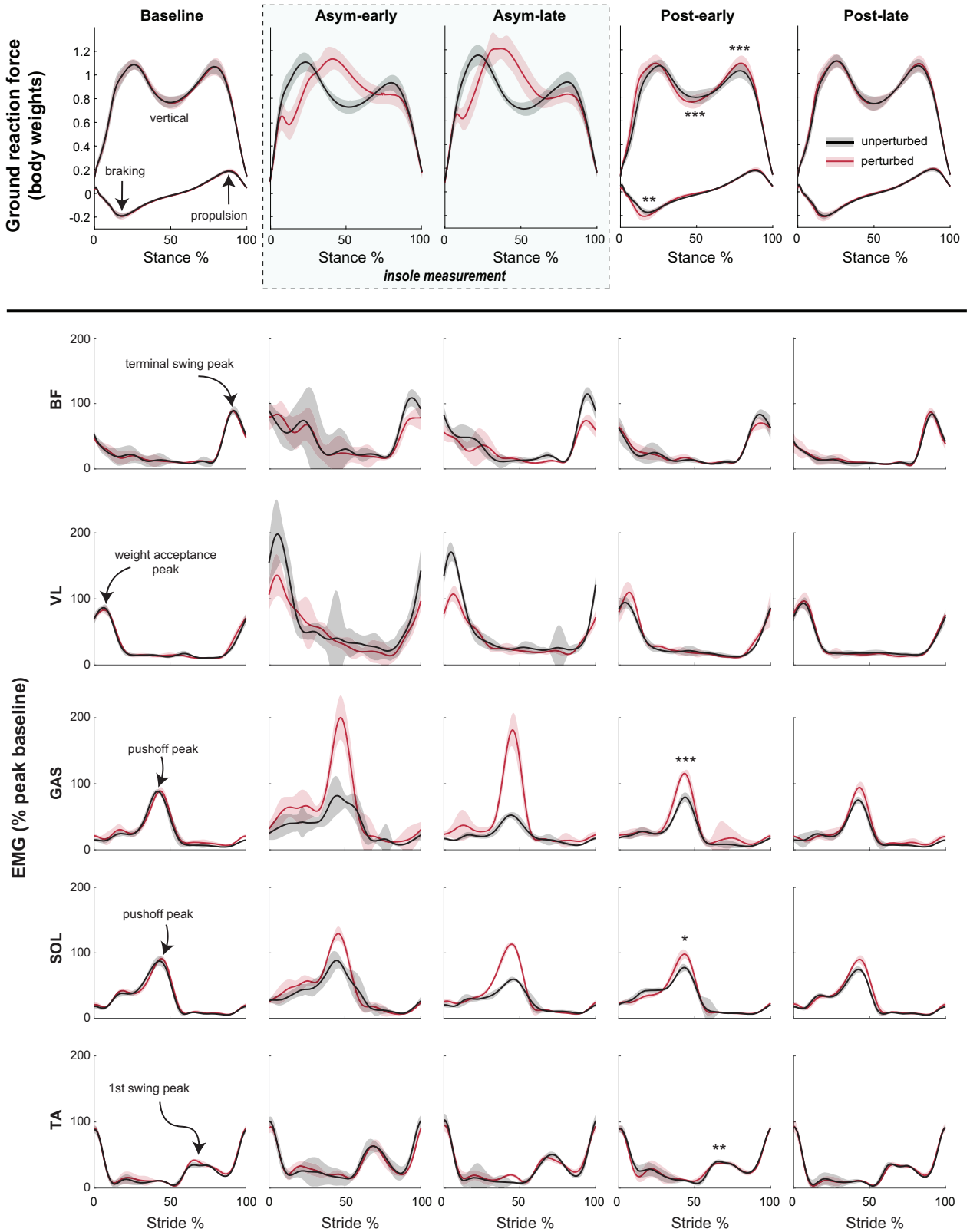

Figure 2. Electromyography (EMG) and ground reaction force (GRF) traces during Baseline, Asym-early, Asym-late, Post-early, and Post-late conditions. Selected measures are illustrated and labeled in the "Baseline" plots. Asterisks reflect significant difference to baseline via paired *t* test: $*P < 0.05$, $**P < 0.01$, $***P < 0.001$.

Downloaded from journals.physiology.org/journal/jn at Univ of Massachusetts (128.119.077.226) on October 26, 2026.

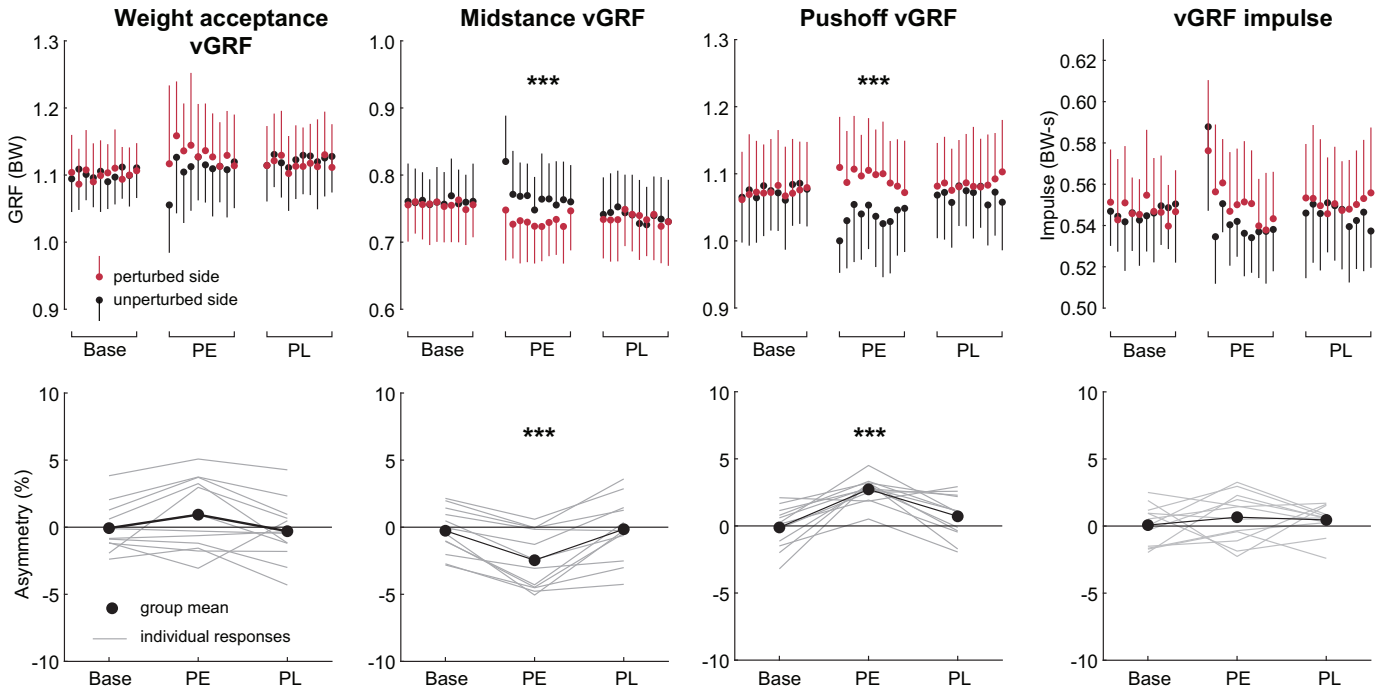

Figure 3. Group means of vertical ground reaction force (GRF) measures per condition (Base = Baseline, PE = Post-early, PL = Post-late) for the perturbed and unperturbed limbs per stride (*top*) and asymmetry ratio (*bottom*). Error bars reflect one standard deviation. Asterisks reflect significant difference to baseline via paired *t* test: ***$P < 0.001$.

observed postperturbation increases in activity for muscles that contribute to push-off (GAS and SOL) on the perturbed side, but did not observe aftereffects in muscles that play a greater role in body support (BF and VL). During the late-asymmetry condition, activity appeared to increase on the unperturbed side while remaining relatively unchanged on the perturbed side for both BF and VL. For the TA, similar responses were observed in both limbs following the adaptation. It is possible that participants adapted to the asymmetric stiffness condition by dorsiflexing on both sides for extra

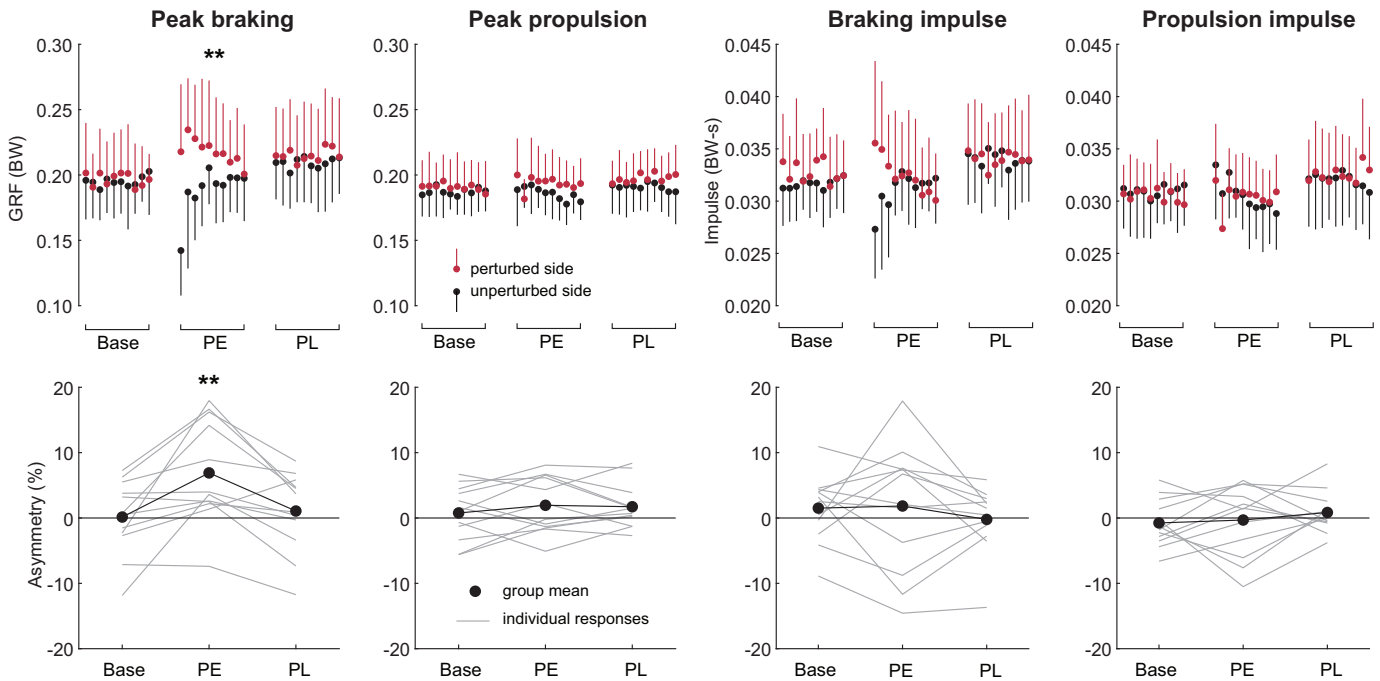

Figure 4. Group means of braking ground reaction force (GRF) and propulsive GRF measures per condition (Base = Baseline, PE = Post-early, PL = Post-late) for the perturbed and unperturbed limbs per stride (*top*) and asymmetry ratio (*bottom*). Error bars reflect one standard deviation. Asterisks reflect significant difference to baseline via paired *t* test: **$P < 0.01$.

Downloaded from journals.physiology.org/journal/jn at Univ of Massachusetts (128.119.077.226) on October 26, 2026.

Table 2. *Muscle excitation outcome measures*

	Baseline	Asym-Early	Asym-Late	Post-Early	Post-Late	Main Effect *P* Value
BF (% Asym)	**0.4 ± 1.0**	**−12.1 ± 13.3**	**−19.9 ± 21.0**	**−4.8 ± 13.4**	**1.8 ± 17.0**	**0.003**
VL (% Asym)	**−0.1 ± 2.5**	**−17.2 ± 17.2**	**−20.3 ± 14.4**	**5.3 ± 13.1**	**2.5 ± 9.8**	**<0.001**
GAS (% Asym)	**−0.8 ± 2.4**	**34.2 ± 18.5**	**47.7 ± 10.2**	**19.9 ± 8.3**	**9.7 ± 8.5**	**<0.001**
SOL (% Asym)	**0.2 ± 0.9**	**13.9 ± 15.4**	**27.2 ± 12.4**	**9.7 ± 8.8**	**8.9 ± 8.0**	**<0.001**
TA (% Asym)	**5.3 ± 8.2**	**−4.1 ± 11.8**	**−6.2 ± 13.8**	**−3.5 ± 10.9**	**−1.3 ± 9.0**	**0.014**

Values are means ± SD. Significant differences ($P < 0.05$) are shown in bold. Positive asymmetry = relatively greater value on the perturbed than the unperturbed side. Negative asymmetry = relatively greater value on the unperturbed than the perturbed side.

toe clearance on both sides of the treadmill. However, further examination of more participants is necessary to show a clear trend in TA adaptation. In contrast, GAS and SOL both appeared to increase on the perturbed side during the perturbation, and that increased activity persisted after the perturbation concluded.

Despite observing significant changes in the transient features of weight bearing (asymmetrical shifts in peak push-off vGRF and minimum midstance vGRF), we did not observe a change in vGRF impulse asymmetry, indicating that the relative contribution of each limb to body support during the full stance phase did not change. We can speculate that this may be because the perturbation we applied is mechanically efficient, despite the magnitude of disruption. For the walking frequencies we observed, the AdjuSST has a frequency-response gain at or slightly above unity (19), meaning that nearly all of the mechanical energy put into the system by a participant's weight is returned by the spring. For participants without neuromotor deficits, adaptation could involve modifying the transient aspects of weight-bearing while maintaining approximate symmetry in overall weight-bearing impulse.

Braking and Propulsion Aftereffects

Asymmetric stiffness walking elicited changes in peak braking force, but not in propulsive force. This finding runs counter to our hypothesis. As previously discussed, however, push-off vGRF and plantar flexor muscle activity shifted toward the perturbed side postperturbation, suggesting that a motor adaptation increasing push-off overall was being elicited, but that the direction of the push-off force vector was aligned vertically. This contradicts a conclusion from Chambers and Artemiadis (17) that increases in peak vGRF at push-off imply increases in propulsion force, underscoring the need to directly measure braking and propulsion ground reaction forces when adaptation in propulsion is a relevant measure. This adaptation may result from the stiffness perturbation being constrained to the vertical direction. Likewise, the significant aftereffect in peak braking force asymmetry is coupled with a lack of significance in weight acceptance vGRF asymmetry, suggesting a more horizontal limb posture at heel-strike. It is possible that to achieve an increase in propulsion, the perturbation could be modified to additionally elicit an adaptation in trailing limb angle or by increasing propulsion demands overall (e.g., by introducing an upward incline) (24). It remains to be seen whether this is the case for walkers with chronic hemiparetic stroke.

In addition, while we found a significant aftereffect in the peak braking force, it appears to rapidly wash out, nearly reaching symmetry within 10 strides (Fig. 4). This rapid washout may be why we did not see a significant effect of condition in braking impulse, in which the first five strides and the last five strides of the post-early condition largely cancel out (Fig. 4).

Spatiotemporal Symmetry Was Unaffected

Despite changes to ground reaction force and muscle excitation symmetry, we did not observe aftereffects in spatiotemporal symmetry. Using data from the force-sensing insoles, we measured a mean shift in stance time toward the unperturbed leg (~1% asymmetry) and an increase in stride time by ~30 ms during the perturbation, but we did not include these measurements in our statistical analysis because those were recorded at a lower temporal resolution and lower force-sensing accuracy than the instrumented treadmill. Regardless of their statistical relevance, these changes are small compared with temporal changes observed during split-belt treadmill training (e.g., ~30% at 4:1 belt speed ratio) (25). This is possibly influenced by the belt speeds being tied in our perturbation, which may constrain the spatiotemporal gait parameters to remain closer to symmetry than if participants were allowed more freedom (i.e., on a self-paced treadmill or overground).

Study Limitations and Future Work

This study investigated the effects of asymmetric stiffness walking on healthy young adults to identify aftereffects indicative of neuromotor adaptation. Although we were able to analyze our measures of interest before and after the perturbation, anterior-posterior GRF, step length, and stride length were not captured during the perturbation. We were able to measure EMG signals at full resolution during the perturbation, but vGRF was measured with force-sensing insoles, which are not a perfect equivalent for the force plates in the rigid instrumented treadmill. Therefore, we included them to qualitatively illustrate the vGRF profile during the perturbation, but did not include them or the temporal measures computed from them in our analyses. Our protocol required the transport of the participant between experimental setups before and after the perturbation. Although we took precautions to prevent participants from taking any steps after exposure to the perturbation, the "Post-early" condition started 1–2 min after exposure. The first stride post-perturbation was also discarded to avoid including effects from the acceleration of the treadmill belts. Therefore, it is possible that the magnitude of the effects on gait immediately postperturbation was not fully captured.

Downloaded from journals.physiology.org/journal/jn at Univ of Massachusetts (128.119.077.226) on October 26, 2026.

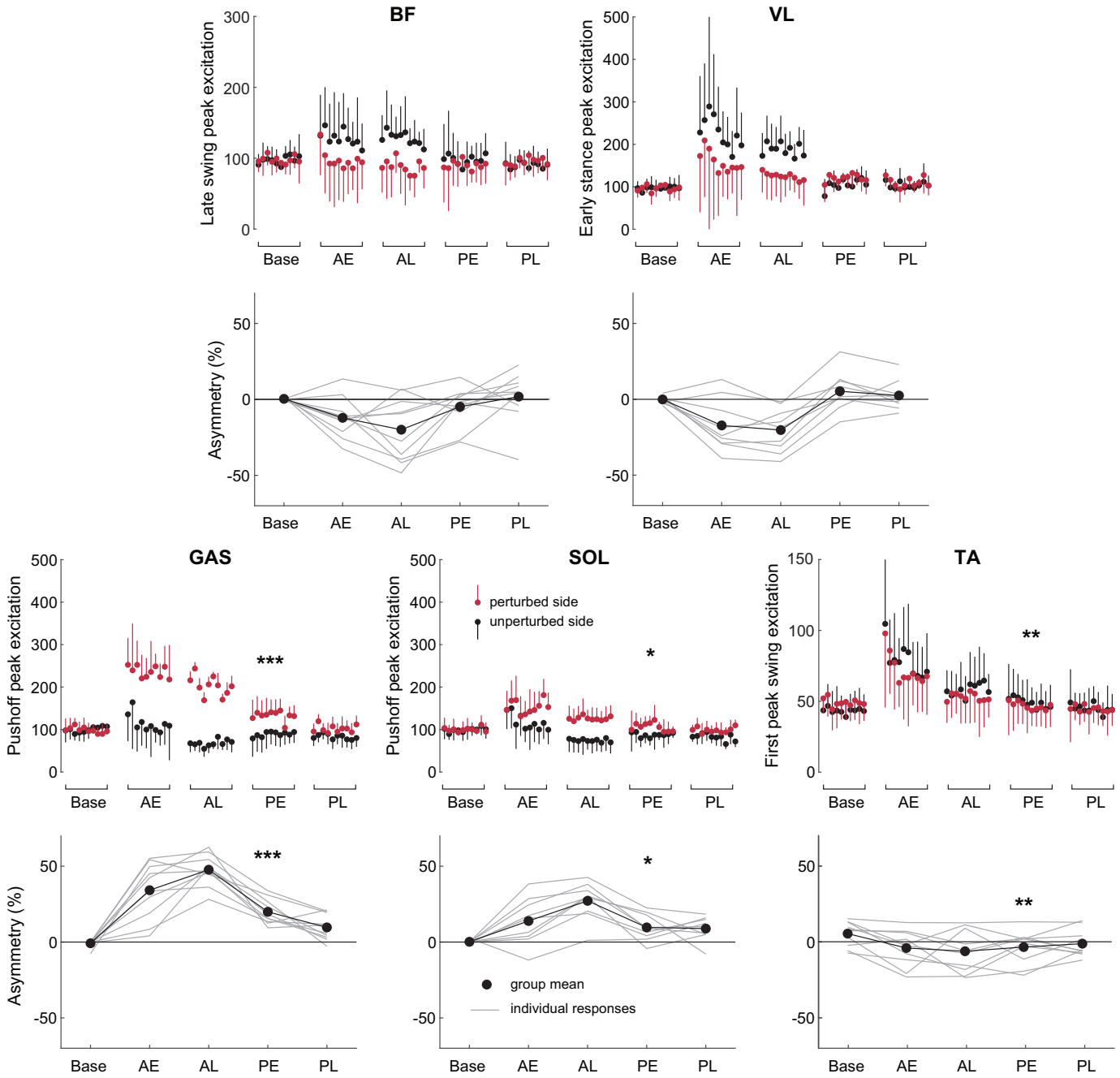

Figure 5. Group means and standard deviations of EMG measures per condition (Base = Baseline, AE = Asym-early, AL = Asym-late, PE = Post-early, PL = Post-late) per stride (*top*) and asymmetry ratio (*bottom*). Error bars reflect one standard deviation. Asterisks reflect significant difference to baseline via paired *t* test: $^{*}P < 0.05$, $^{**}P < 0.01$, $^{***}P < 0.001$.

Finally, it is likely that the magnitude of the perturbation experienced by each participant is dependent on their height and weight. We chose to present a single stiffness perturbation to characterize the group response to this fixed measure, but hope to better understand how the perturbation may be personalized as we obtain more data with different stiffness values.

A limitation inherent to the analysis of behavioral effects is that our conclusions about neural changes to motor control are indirect interpretations of our observations. This limitation can be addressed in part by replicating experimental results with neuromuscular models in which the mechanisms for motor control are fully described. In prior work, we used optimal control predictive simulations to describe split-belt treadmill walking (26), and more recently, to predict asymmetric stiffness walking to a wide range of mechanical parameters (27), in which many of the predicted changes to vGRF magnitude and muscle activity asymmetry were borne out in these experiments. Refinement of neuromuscular simulations focused on interpretation of our experimental findings will be an avenue for future work.

Downloaded from journals.physiology.org/journal/jn at Univ of Massachusetts (128.119.077.226) on October 26, 2026.

Finally, while insights into adaptation to asymmetric stiffness walking in healthy young adults are useful, they do not necessarily generalize to hemiparetic gait. As in the development of split-belt treadmill training, this work quantifies the effect of the intervention in a healthy control population (11), a necessary step in the process of understanding the mechanisms that may eventually be leveraged toward clinical applications (10). We will investigate the effects of this intervention in individuals with chronic stroke in future.

Conclusions

Asymmetric stiffness walking elicited changes to push-off GRF asymmetry corresponding with changes to plantar flexor activity, indicating a neuromotor adaptation to the perturbation. In contrast to split-belt treadmill perturbations, it did not elicit changes to spatiotemporal parameters of gait. Furthermore, while vertical GRF shifted toward the perturbed side limb during push-off, weight-bearing impulse over the stance phase and propulsive force did not. Further study is needed to determine if asymmetric stiffness walking can elicit improved symmetry in push-off GRF in individuals with chronic stroke.

DATA AVAILABILITY

The data supporting the findings of this study are openly available in Figshare at https://doi.org/10.6084/m9.figshare.31290160.

SUPPLEMENTAL MATERIAL

Supplemental Figs. S1 and S2: https://doi.org/10.6084/m9.figshare.30813083.

GRANTS

This study was supported by NIH R21 EB033450, awarded to M.E.H. and W.H., UMass Amherst ADVANCE Collaborative Research Award, awarded to ME.H. and W.H., UMass Amherst Institute of Applied Life Sciences (IALS) Midi Grant, awarded to M.E.H. and W.H., and ACSM Foundation Early Career Research Grant, awarded to W.H.

DISCLOSURES

No conflicts of interest, financial or otherwise, are declared by the authors.

AUTHOR CONTRIBUTIONS

M.P., M.E.H., and W.H. conceived and designed research; M.P., E.G.S., J.M.J., J.M.C., and L.C.M. performed experiments; M.P., E.G.S., J.M.J., J.M.C., and L.C.M. analyzed data; M.P., E.G.S., J.M.J., J.M.C., L.C.M., and W.H. interpreted results of experiments; M.P., E.G.S., and J.M.J. prepared figures; M.P., E.G.S., and W.H. drafted manuscript; M.P., E.G.S., M.E.H., and W.H. edited and revised manuscript; M.P., E.G.S., J.M.J., J.M.C., L.C.M., M.E.H., and W.H. approved final version of manuscript.

REFERENCES

1. **Xu J**, **Witchalls J**, **Preston E**, **Pan L**, **Waddington G**, **Adams R**, **Han J.** Stroke-related factors associated with gait asymmetry in ambulatory stroke survivors: a systematic review and meta-analysis. *Gait Posture* 121: 173–181, 2025. doi:10.1016/j.gaitpost.2025.05.010.
2. **Fling BW**, **Curtze C**, **Horak FB.** Gait asymmetry in people with Parkinson's disease is linked to reduced integrity of callosal sensorimotor regions. *Front Neurol* 9: 215, 2018. doi:10.3389/fneur.2018.00215.
3. **Hagen AC**, **Acosta JS**, **Geltser CS**, **Fling BW.** Split-belt treadmill adaptation improves spatial and temporal gait symmetry in people with multiple sclerosis. *Sensors (Basel)* 23: 5456, 2023. doi:10.3390/s23125456.
4. **Gardinier ES**, **Manal K**, **Buchanan TS**, **Snyder-Mackler L.** Gait and neuromuscular asymmetries after acute anterior cruciate ligament rupture. *Med Sci Sports Exerc* 44: 1490–1496, 2012. doi:10.1249/MSS.0b013e31824d2783.
5. **Constantinou M**, **Barrett R**, **Brown M**, **Mills P.** Spatial-temporal gait characteristics in individuals with hip osteoarthritis: a systematic literature review and meta-analysis. *J Orthop Sports Phys Ther* 44: 291–2B7, 2014. doi:10.2519/jospt.2014.4634.
6. **Roelker SA**, **Bowden MG**, **Kautz SA**, **Neptune RR.** Paretic propulsion as a measure of walking performance and functional motor recovery post-stroke: a review. *Gait Posture* 68: 6–14, 2019. doi:10.1016/j.gaitpost.2018.10.027.
7. **Li W**, **Li Y**, **Gao Q**, **Liu J**, **Wen Q**, **Jia S**, **Tang F**, **Mo L**, **Zhang Y**, **Zhai M**, **Chen Y**, **Guo Y**, **Gong W.** Change in knee cartilage components in stroke patients with genu recurvatum analysed by zero TE MR imaging. *Sci Rep* 12: 3751, 2022. doi:10.1038/s41598-022-07817-w.
8. **Jørgensen L**, **Jacobsen BK**, **Wilsgaard T**, **Magnus JH.** Walking after stroke: does it matter? Changes in bone mineral density within the first 12 months after stroke. A longitudinal study. *Osteoporos Int* 11: 381–387, 2000. doi:10.1007/s001980070103.
9. **Rantakokko M**, **Mänty M**, **Rantanen T.** Mobility decline in old age. *Exerc Sport Sci Rev* 41: 19–25, 2013. doi:10.1097/JES.0b013e3182556f1e.
10. **Reisman DS**, **McLean H**, **Keller J**, **Danks KA**, **Bastian AJ.** Repeated split-belt treadmill training improves poststroke step length asymmetry. *Neurorehabil Neural Repair* 27: 460–468, 2013. doi:10.1177/1545968312474118.
11. **Reisman DS**, **Block HJ**, **Bastian AJ.** Interlimb coordination during locomotion: what can be adapted and stored? *J Neurophysiol* 94: 2403–2415, 2005. doi:10.1152/jn.00089.2005.
12. **Awad LN**, **Lewek MD**, **Kesar TM**, **Franz JR**, **Bowden MG.** These legs were made for propulsion: advancing the diagnosis and treatment of post-stroke propulsion deficits. *J Neuroeng Rehabil* 17: 139, 2020. doi:10.1186/s12984-020-00747-6.
13. **Lewek MD**, **Braun CH**, **Wutzke C**, **Giuliani C.** The role of movement errors in modifying spatiotemporal gait asymmetry post stroke: a randomized controlled trial. *Clin Rehabil* 32: 161–172, 2018. doi:10.1177/0269215517723056.
14. **Santucci V**, **Alam Z**, **Liu J**, **Spencer J**, **Faust A**, **Cobb A**, **Konantz J**, **Eicholtz S**, **Wolf S**, **Kesar TM.** Immediate improvements in post-stroke gait biomechanics are induced with both real-time limb position and propulsive force biofeedback. *J Neuroeng Rehabil* 20: 37, 2023. doi:10.1186/s12984-023-01154-3.
15. **Hinton EH**, **Buffum R**, **Kingston D**, **Stergiou N**, **Kesar T**, **Bierner S**, **Knarr BA.** Real-time visual kinematic feedback during overground walking improves gait biomechanics in individuals post-stroke. *Ann Biomed Eng* 52: 355–363, 2024. doi:10.1007/s10439-023-03381-0.
16. **Kal E**, **Winters M**, **van der Kamp J**, **Houdijk H**, **Groet E**, **van Bennekom C**, **Scherder E.** Is implicit motor learning preserved after stroke? A systematic review with meta-analysis. *PLoS One* 11: e0166376, 2016. doi:10.1371/journal.pone.0166376.
17. **Chambers V**, **Artemiadis P.** Using robot-assisted stiffness perturbations to evoke aftereffects useful to post-stroke gait rehabilitation. *Front Robot AI* 9: 1073746, 2022. doi:10.3389/frobt.2022.1073746.
18. **Winter DA.** *The biomechanics and motor control of human gait*. University of Waterloo Press, 1987. doi:10.1002/9780470549148.
19. **Price M**, **Locurto D**, **Abdikadirova B**, **Huber ME**, **Hoogkamer W.** Design and characterization of the AdjuSST: an adjustable surface stiffness treadmill. *IEEE/ASME Trans Mechatron*, 30: 4754–4765, 2025. doi:10.1109/TMECH.2024.3508476.
20. **Shiavi R**, **Frigo IC**, **Pedotti A.** Electromyographic signals during gait: criteria for envelope filtering and number of strides. *Med Biol Eng Comput* 36: 171–178, 1998. doi:10.1007/BF02510739.
21. **Emanuel Singh R**, **Iqbal K**, **White GK**, **Holtz J.** A review of EMG techniques for detection of gait disorders. In: *Artificial Intelligence - Applications in Medicine and Biology*. IntechOpen, 2019. doi:10.5772/intechopen.84403.

Downloaded from journals.physiology.org/journal/jn at Univ of Massachusetts (128.119.077.226) on October 26, 2026.

22. **Lamontagne A**, **Malouin F**, **Richards CL**, **Dumas F.** Mechanisms of disturbed motor control in ankle weakness during gait after stroke. *Gait Posture* 15: 244–255, 2002. doi:10.1016/S0966-6362(01)00190-4.
23. **Kamphuis JF**, **De Kam D**, **Geurts ACH**, **Weerdesteyn V.** Is weight-bearing asymmetry associated with postural instability after stroke? A systematic review. *Stroke Res Treat:* 2013: 692137, 2013. doi:10.1155/2013/692137.
24. **Sombric CJ**, **Torres-Oviedo G.** Augmenting propulsion demands during split-belt walking increases locomotor adaptation of asymmetric step lengths. *J Neuroeng Rehabil* 17: 69, 2020. doi:10.1186/s12984-020-00698-y.
25. **Stenum J**, **Choi JT.** Step time asymmetry but not step length asymmetry is adapted to optimize energy cost of split-belt treadmill walking. *J Physiol* 598: 4063–4078, 2020. doi:10.1113/JP279195.
26. **Price M**, **Huber ME**, **Hoogkamer W.** Minimum effort simulations of split-belt treadmill walking exploit asymmetry to reduce metabolic energy expenditure. *J Neurophysiol* 129: 900–913, 2023. doi:10.1152/jn.00343.2022.
27. **Price M**, **Abdikadirova B**, **Hoogkamer W**, **Huber ME.** Forward simulations of walking on surfaces with asymmetric mechanical impedance: insights for gait rehabilitation. *Annu Int Conf IEEE Eng Med Bio Soc* 2025: 1–7, 2025. doi:10.1109/EMBC58623.2025.11254074.

Downloaded from journals.physiology.org/journal/jn at Univ of Massachusetts (128.119.077.226) on October 26, 2026.